Title
A COMPARISON TO THEORY OF OBSERVED STABILITY FAILURES OF THIN SPHERICAL SHELLS

Author
Cook, Garth E.

Publication Date
1958-08-08

UCRL8403

UNIVERSITY OF CALIFORNIA
Ernest O. Lawrence
Radiation Laboratory

A COMPARISON TO THEORY OF OBSERVED STABILITY FAILURES OF THIN SPHERICAL SHELLS

DISCLAIMER

UCRL-8403
Physics and Mathematics

UNIVERSITY OF CALIFORNIA

Lawrence Radiation Laboratory
Berkeley, California

Contract No. W-7405-eng-48

A COMPARISON TO THEORY OF OBSERVED STABILITY FAILURES OF THIN SPHERICAL SHELLS

Garth E. Cook

August 8, 1958

Printed for the U. S. Atomic Energy Commission

Printed in USA. Price 75 cents. Available from the
Office of Technical Services
U. S. Department of Commerce
Washington 25, D. C.

A COMPARISON TO THEORY OF OBSERVED STABILITY FAILURES OF THIN SPHERICAL SHELLS

Garth E. Cook

Lawrence Radiation Laboratory
University of California
Berkeley, California

August 8, 1958

ABSTRACT

Experimental data on stability failures of thin spherical-shell metal windows show that the windows fail at approximately one-third the pressure calculated by the classical theory of S. Timoshenko. The experimental data are seen to compare closely with the results calculated by the newer theories of Von Karman and Tsien.

A COMPARISON TO THEORY OF OBSERVED STABILITY FAILURES OF THIN SPHERICAL SHELLS

Garth E. Cook*

Lawrence Radiation Laboratory
University of California
Berkeley, California

August 8, 1958

INTRODUCTION

The experimental data and comparison to theory contained in this paper were obtained during the design of an experiment in which a liquid hydrogen target was to be bombarded by a beam of nuclear particles. The liquid hydrogen was contained in a stainless-steel tank surrounded by a vacuum jacket, as shown in Fig. 1. Because of the explosive nature of hydrogen, it was necessary to design the windows at the end of the jacket and tank to withstand at least 160 psi on the concave side and 35 psi on the convex side of each window. Other design requirements limited the spherical radius of the windows to between 7-1/2 and 10 inches and the material to type-310 or 305 stainless steel. The critical design criterion was the 35-psi external load.

In order to reduce the beam attenuation, it was desirable to make these windows as thin as possible. Consequently, they were designed using the classical theory of stability failure of S. Timoshenko.[1] Figure 2 shows a thin spherical shell subjected to a uniform external pressure, P. At a certain critical pressure, P_{cr}, the shell becomes unstable and large deformations occur. According to Timoshenko, the value of P_{cr} at which this buckling should occur is:

$$P_{cr} = 1.212\, E \left(\frac{t}{R} \right)^2 , \qquad (1)$$

---

*Presently with Guided Missiles Division, Firestone Tire and Rubber Co., Monterey, California.

where

$$\sigma_{cr} = \frac{P_{cr} R}{2t}$$

and

$$\frac{\sigma_{cr} R}{Et} = \frac{1}{\sqrt{3(1-\mu^2)}} \quad .$$

The symbols used above are defined as follows:

P_{cr} = critical or buckling pressure

σ_{cr} = critical or buckling stress

E = modulus of elasticity of the shell

t = shell thickness

R = radius of curvature

μ = Poisson's ratio (0.3) .

Upon trial the windows failed at approximately one-third the expected value of P_{cr}. As a consequence, a series of tests was made in which the parameters of thickness and spherical radius were changed. The data obtained from these tests revealed that the buckling load is only one-third to one-fourth that calculated by Timoshenko's equations. The experimental results were found to be consistent with the newer theories of Von Karman and Tsien.[2]

DISCUSSION OF THEORY

Buckling Criteria

The mechanism of stability or buckling-type failures in a shell or structure may be understood by an examination of the energy in the structure. For a system to be in stable equilibrium, the total energy of the system must be a minimum; that is, there must be no deflected position of the structure in which the total energy of the structure is less than in the undeflected position.

This can be simply demonstrated by considering a vertical-beam column. Let ΔV be the strain energy of bending of the column, and ΔT denote the work done by the load in bending the column. The column will be stable if $\Delta V - \Delta T > 0$. In other words, more energy is required to bend the beam than is released by the loss in potential energy because of the weight moving downward. It can therefore be seen that more energy is required to keep the beam in its deflected shape than in its undeflected shape.

If unrestrained, the beam will snap back into its normal undeflected position when the load is removed. By similar reasoning it can be seen that the condition for instability is that $\Delta V - \Delta T < 0$, because less energy is required to keep the beam deflected than undeflected. In this case the beam will continue to deflect until such a position that the beam is again in stable equilibrium, if such occurs before complete collapse.

It is seen from the above that the criterion for incipient failure is $\Delta V = \Delta T$. This case is commonly known as neutral stability. If expressions for the energy are written in terms of the critical load, the criterion $\Delta V = \Delta T$ can be used to find the load at which buckling occurs.

Application to Spherical Shells

To describe more accurately the mechanism of stability failures of thin spherical shells, Th. Von Karman and Hsue-Shen Tsien of the California Institute of Technology formulated the following theory:[2] Suppose a gradually increasing pressure (below the critical pressure) is applied to the ideal shell shown in Fig. 2. If continuous external pressure-deflection readings are taken and plotted, a curve similar to

Fig. 3 results. Curve 1, A_1, B_1 corresponds to the case of an extremely thin shell with no bending stiffness. This curve has five points of interest: points 1 and 3 are in stable equilibrium; point 2 is in unstable equilibrium; points A_1 and B_1 are in neutral equilibrium. The point of incipient failure is at A_1. Any load condition of the shell corresponding to a point to the left of A_1 is stable and not subject to stability failures. Curves 1, A_2, B_2 and 1, A_3, B_3 correspond to the cases of finite bending stiffness of progressively greater magnitude.

In an actual shell having initial imperfections in shape and which is subjected to vibration and shock, point A might never be reached. Instead, the failing load noted in the laboratory actually corresponds to the minimum load at point B.

If it can be shown that there are shapes not far from the spherical which involve a lower level of energy, and that the shell jumps to these positions before the peak at point A is reached, then a more reasonable and accurate description of stability failures can be obtained. Von Karman and Tsien have done just this. Their solution gives the following equations:

$$\frac{\sigma_{cr} R}{Et} = \frac{4}{5}\left[\sqrt{\frac{16}{7}\left(\frac{\delta}{t}\right)^2 + \frac{10}{3}} - \frac{3}{2}\left(\frac{\delta}{t}\right)\right] \qquad (2)$$

and

$$\beta^2 = \sqrt{\frac{16}{7}\left(\frac{\delta}{t}\right)^2 + \frac{10}{3}\left(\frac{t}{R}\right)^2}, \qquad (3)$$

where δ is the deflection of the shell and β is the semiangular extent of the buckle. Equation 2 is plotted in Fig. 4. The minimum value of $\sigma_{cr} R/Et$ is approximately equal to 0.183, as seen in Fig. 4. This means that the minimum load required to keep the shell in its deflected position is $P_{cr} = 2(0.183)E(t/R)^2$, which occurs for a deflection of about 10 times the thickness. The value of β corresponding to the minimum load occurs at $\beta = 3.82\sqrt{t/R}$. The important point to note from Fig. 4, however, is that such a minimum point does exist and that the design of the windows could be based on this minimum stress or load.

An examination of Von Karman and Tsien's derivation of the above equations (Eqs. 2 and 3) reveals that they have made four assumptions:

a. The solid angle (2β of Fig. 2) of the deflected portion is small.

b. The deformation is rotationally symmetrical.

c. The deflection of any element of the shell is parallel to the axis of rotational symmetry.

d. Poisson's ratio is zero.

Assumption (a) was experimentally noted by the present author; however data could not be taken, because the initial buckle propagated rapidly and soon became a plastic failure. The accuracy of assumptions (b) and (c) is more difficult to assess. A somewhat different effect has been observed by the present author. Some of the experimental shells failed along the sloping sides, and in general, the buckle was not rotationally symmetrical. A possible explanation of this phenomenon lies in the fact that some of the shells were spun from flat sheet stock. The deepest draw was in the sloping sides, which reduced the thickness in this area by about 10%. The critical load would be felt in this portion of the shell before it was felt at the center of symmetry. Assumption (d) probably has little effect.

Another new theory of failure was derived by Hsue-Shen Tsien,[3] using as a basis the paper which he co-authored with Von Karman,[2] as well as a later work by K.O. Friedrichs.[4] The result of Tsien's solution gives the following equation:

$$\frac{\sigma_{cr} R}{Et} = \frac{1}{2}\sqrt{\frac{16}{5}\left(\frac{1}{1-\mu^2}\right) + \frac{32}{35}\left(\frac{\delta}{t}\right)^2} - \frac{1}{2}\left(\frac{\delta}{t}\right). \tag{4}$$

This equation is plotted in Fig. 5. This plot is analogous to Fig. 4. It is interesting to note that the minimum point in Fig. 4, which was the basis of the solution by Von Karman and Tsien, is missing in Fig. 5.

The final result of Tsien's solution lies in the following equations, in which the subscript 1 refers to conditions at the beginning of buckling, and subscript 2 refers to conditions at the end of buckling:

$$\frac{\sigma_1 R}{Et} = \frac{4}{3(1-\mu^2)} \frac{t}{R\beta^2} + \frac{37}{480} \frac{\beta^2 R}{t} - \frac{3}{32} \frac{\lambda t/R}{1-\mu} \frac{\beta^4 R^2}{t^2} -$$

$$\frac{\beta^2 R}{24t} \left[1 - \frac{\lambda t/R}{(1-\mu)} \frac{\beta^2 R}{t}\right] \sqrt{\left(\frac{7}{4}\right)^2 - \frac{7\lambda t/R}{(1-\mu)} \frac{\beta^2 R}{t}} \qquad (5)$$

and

$$\frac{\sigma_2 R}{Et} = \frac{4}{3(1-\mu^2)} \frac{t}{R\beta^2} + \frac{37}{480} \frac{\beta^2 R}{t} - \frac{1}{6} \frac{\lambda t/R}{1-\mu} \frac{\beta^4 R^2}{t^2} -$$

$$\frac{\beta^2 R}{24t} \sqrt{\left(\frac{7}{4}\right)^2 - \frac{7\lambda t/R}{(1-\mu)} \frac{\beta^2 R}{t}}, \qquad (6)$$

where

$$\lambda = \frac{\text{area of hemisphere}}{\text{area of spherical-shell segment.}}$$

Equations 5 and 6 are plotted against the dimensionless ratio $\beta^2 R/t$ for given values of $\lambda t/R$. A minimum point for $\sigma_1 R/Et$ is found and is labeled $\sigma_{cr1} R/Et$. These values of $\sigma_{cr1} R/Et$ are plotted as a function of $R/\lambda t$ in Fig. 6 with corresponding $\sigma_{cr2} R/Et$.

EXPERIMENTAL RESULTS

The experimental arrangement for testing the hydrogen-tank windows is shown in Fig. 7, and for testing the vacuum-jacket windows in Fig. 8. The loading of the shell was accomplished by hydrostatic pressure controlled by a valve. A Bourdon gage gave pressure indications. In general, the procedure was to increase the pressure until the first buckle was noted. This is referred to as the "failing load" in Table I, which summarizes the experimental results.

Figures 9, 10, and 11 are photographs of the shells. Figure 12 gives the dimensions of each shell.

Table I

Experimental Results and Calculations

	shell number	outside diam (in.)	spherical radius (in.)	thickness (in.)	material-stainless steel (type)	failing load (psi)	classical theory (psi)	Von Karman and Tsien's solution (psi)	Tsien's solution: start of buckling (psi)	Tsien's solution: end of buckling (psi)
spun and machined	1	8	10	.010	309	10	36.4	10.8	17.1	6.9
	2	8	10	.012	309	15	52.5	15.7	26.0	10.3
	3	8	10	.015	309	28	82.0	24.6	42.4	16.2
spun	4	10	10	.010	302	10	36.4	10.8	16.2	6.9
	5	10	10	.018	302	22	118	35.6	54.5	22.3
	6[a]	10	7-1/2	.010	302	6.5	64.6	19.5	28.7	12.2
	7[a]	10	7-1/2	.015	302	13.6	146	42.7	64.9	27.6
	8	10	7-1/2	.018	305	Did not fail at 50 psi	210	63.4	72.9	31.0

[a]These spinnings were defective - wrinkled in spinning

SAMPLE CALCULATION

This sample calculation is for shell No. 1, with the following conditions being assumed:

$E = 30 \times 10^6$ psi

$R = 10$ in.

$t = 0.010$ in.

diameter of the spherical segment = 7.5 in.

The value of P'_{cr} is calculated for each theory, as follows:

Classical Theory[1]

$$P_{cr} = 1.212\, E(t/R)^2$$
$$= 1.212\, (30 \times 10^6)\, (0.010/10)^2$$
$$= 36.4 \text{ psi}$$

Von Karman and Tsien's Theory[2]

$$P_{cr} = 0.366\, E(t/R)^2$$
$$= 0.366\, (30 \times 10^6)\, (0.010/10)^2$$
$$= 10.8 \text{ psi}$$

Tsien's Theory[3] (see Fig. 13)

$$\lambda = \frac{\text{area of hemisphere}}{\text{area of spherical segment}}$$
$$= 1/1-\cos\theta .$$

From the conditions given above, sin θ equals 3.75/10, or 0.375. Therefore, θ equals 22° 1', and cos θ equals 0.927. Consequently we obtain

$$\lambda = 1/1-0.927$$
$$= 13.7$$

We write

$$R/\lambda t = 10/13.7(0.010)$$
$$= 73.$$

Consulting Fig. 6, for a value of $R/\lambda t = 73$ we find corresponding values as follows:

$$\sigma_{cr1}/Et = 0.285$$
$$\sigma_{cr2}/Et = 0.115.$$

Therefore, to find the start of buckling, we write

$$P_{cr1} = 2(0.285)E(t/R)^2$$
$$= 2(0.285)\ (30 \times 10^6)\ (0.010/10)^2$$
$$= 17.1 \text{ psi}.$$

To find the end of buckling, we write

$$P_{cr2} = 2(0.115)E(t/R)^2$$
$$= 2(0.115)(30 \times 10^6)\ (0.010/10)^2$$
$$= 6.9 \text{ psi}.$$

CONCLUSIONS

It should be noted from Table I that the actual buckling load is less than that predicted by the classical equations by at least a factor of three. The equations derived by Von Karman and Tsien fit most closely the experimental data. The equations due solely to Tsien predict the range in which failures occur, although the upper critical load shown in Table I is higher in all cases than the actual failing load.

The influence of initial imperfections is also shown in Table I for shells No. 6 and 7. The imperfections consisted of small flattened areas about 3/4 in. in diameter, circumferentially spaced around the shell at the juncture of the curved surface and the flange above the 1/2-in. fillet. These imperfections had the effect of lowering the buckling pressure by a factor of 3 below Von Karman and Tsien's equation and a factor of almost 10 below the classical equation.

From the experimental data, the closest prediction for thin-shell failures is:

$$\sigma_{cr}R/Et = 0.183$$

or

$$P = 0.366\ E(t/R)^2.$$

ACKNOWLEDGMENT

This work was performed under the auspices of the U.S. Atomic Energy Commission.

REFERENCES

1. S. Timoshenko, Theory of Elastic Stability (McGraw-Hill, New York, 1936).
2. (a) Th. Von Karman and Hsue-Shen Tsien, The Buckling of Spherical Shells by External Pressure, J. Aeronaut. Sci. 7, 43-50 (Dec. 1939).
   (b) Th. Von Karman, Hsue-Shen Tsien, and L.G. Dunn, The Influence of Curvature on the Buckling Characteristics of Structure, J. Aeronaut. Sci. 7, 276-289 (May 1940).
3. Hsue-Shen Tsien, A Theory for the Buckling of Thin Shells, J. Aeronaut. Sci. 9, 373-384 (Aug. 1942).
4. K.O. Freidrichs, On the Minimum Buckling Loads for Thin Spherical Shells, Theodore Von Karman Anniversary Volume (Cal. Tech., Pasadena, 1941), pp. 258-272.

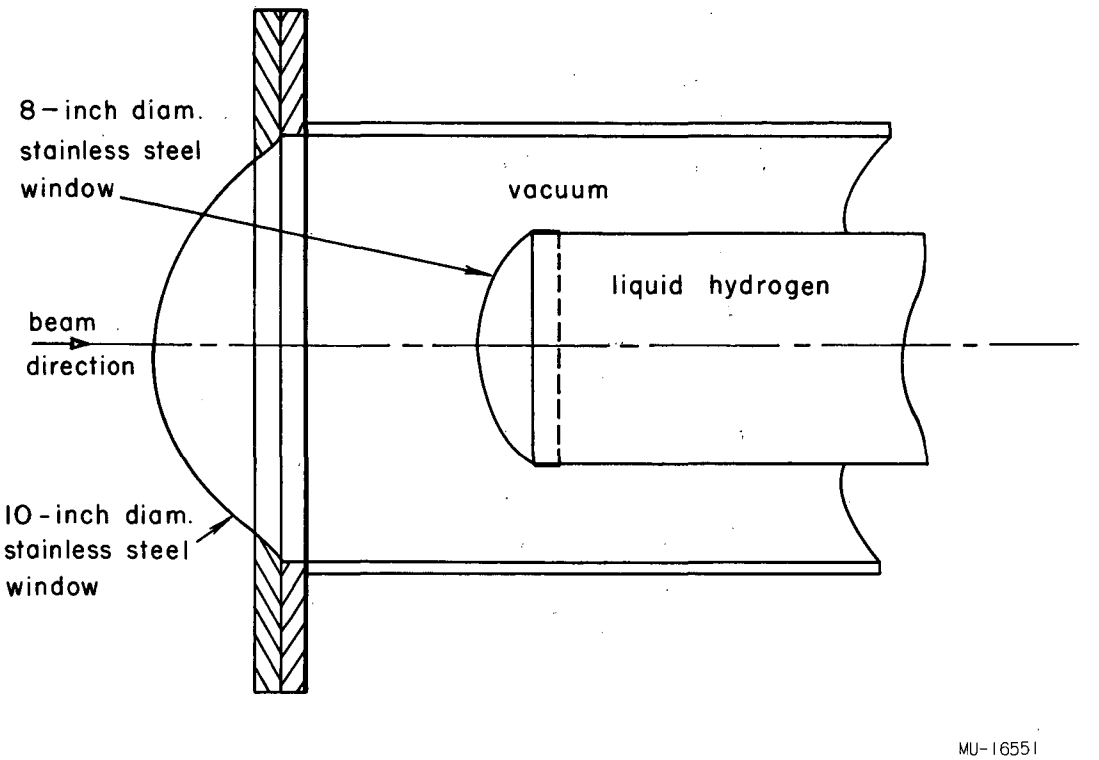

Fig. 1 Arrangement of liquid hydrogen target.

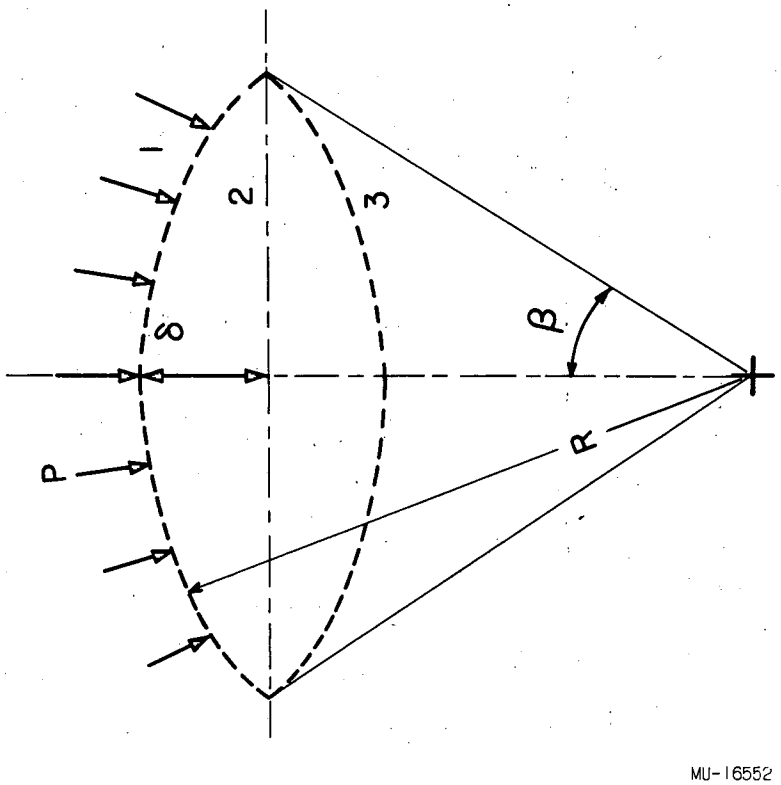

Fig. 2. Thin spherical shell subjected to external pressure P.

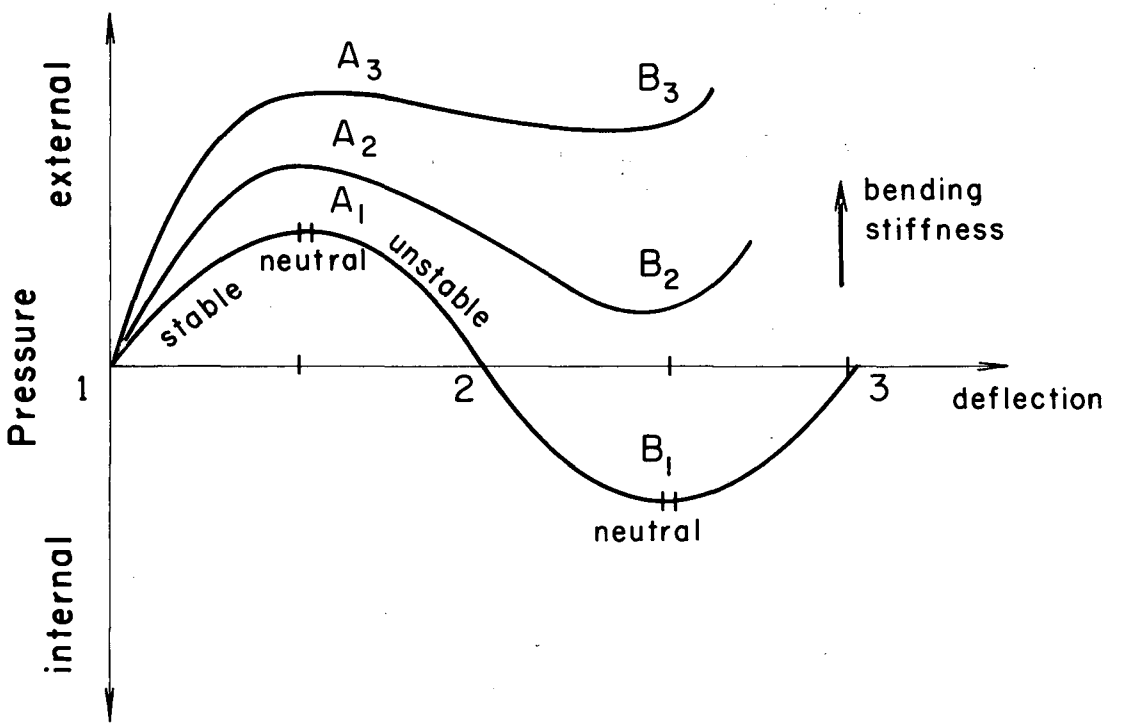

Fig. 3. Pressure required for equilibrium deflection.

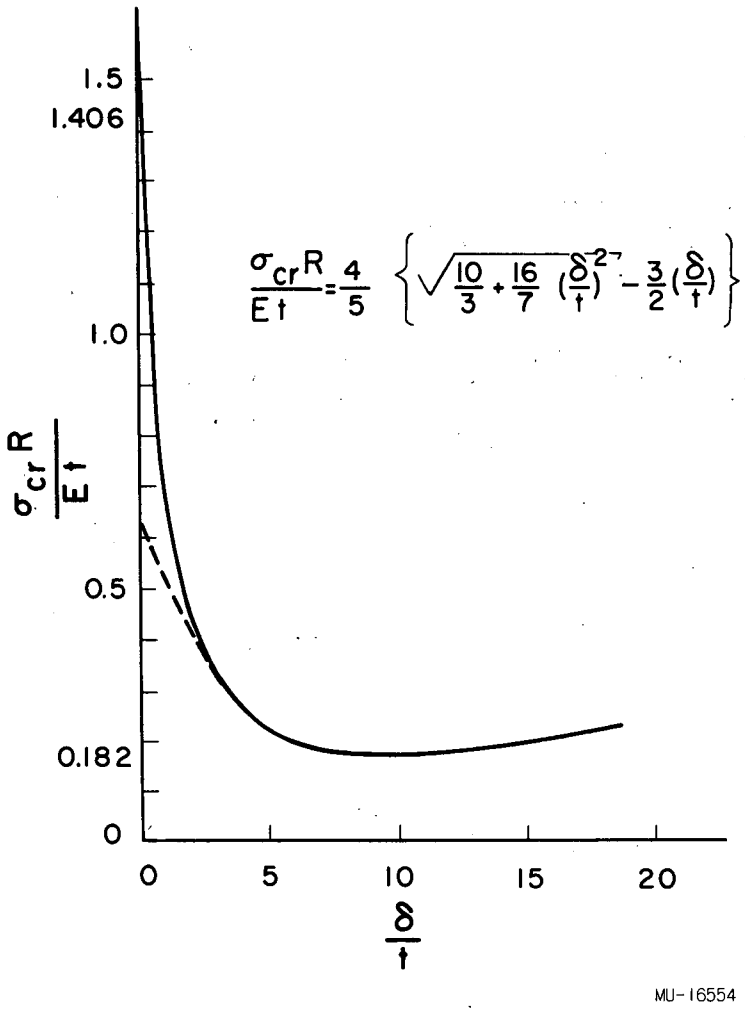

Fig. 4. Compressive stress vs deflection (in dimensionless ratios) as derived by Von Karman and Tsien for the critical buckling stress of a thin spherical shell.

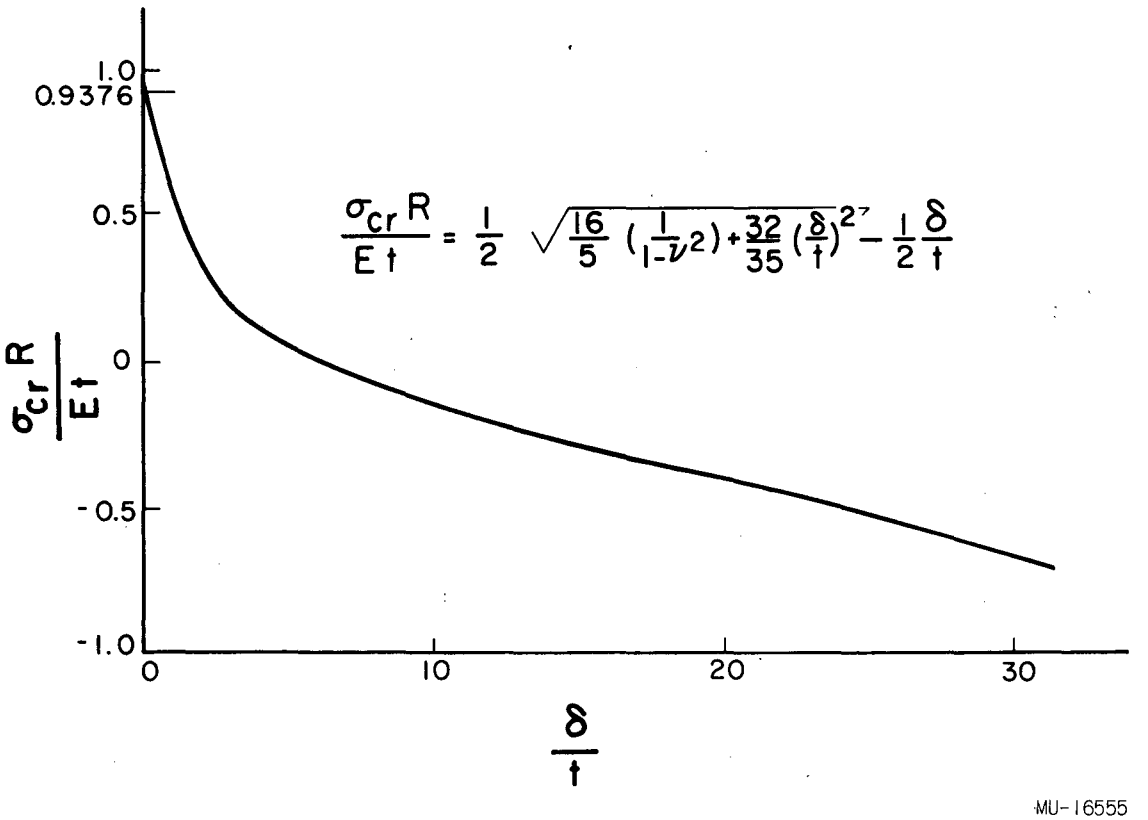

Fig. 5. Compressive stress vs deflection (in dimensionless ratios) as derived by Tsien for the critical buckling stress of a thin spherical shell.

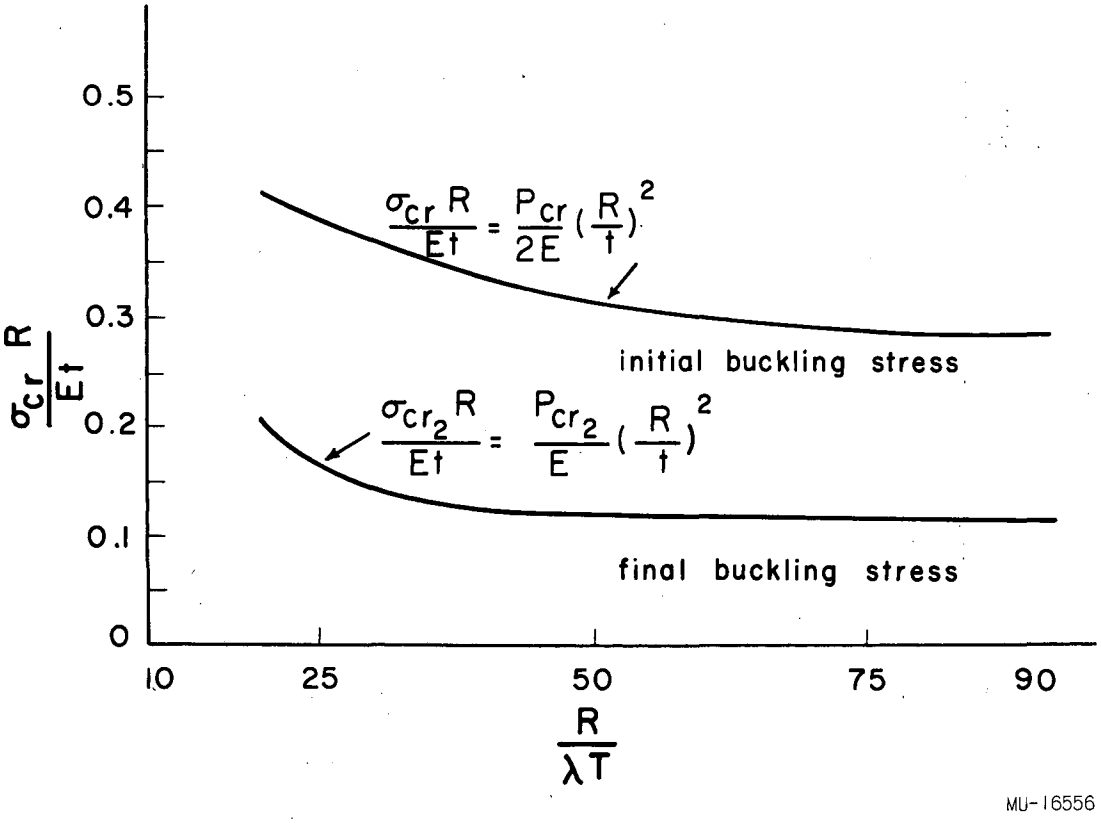

Fig. 6. Initial and final buckling stress of a thin spherical shell as a function of the dimensionless radius, as derived by Tsien.

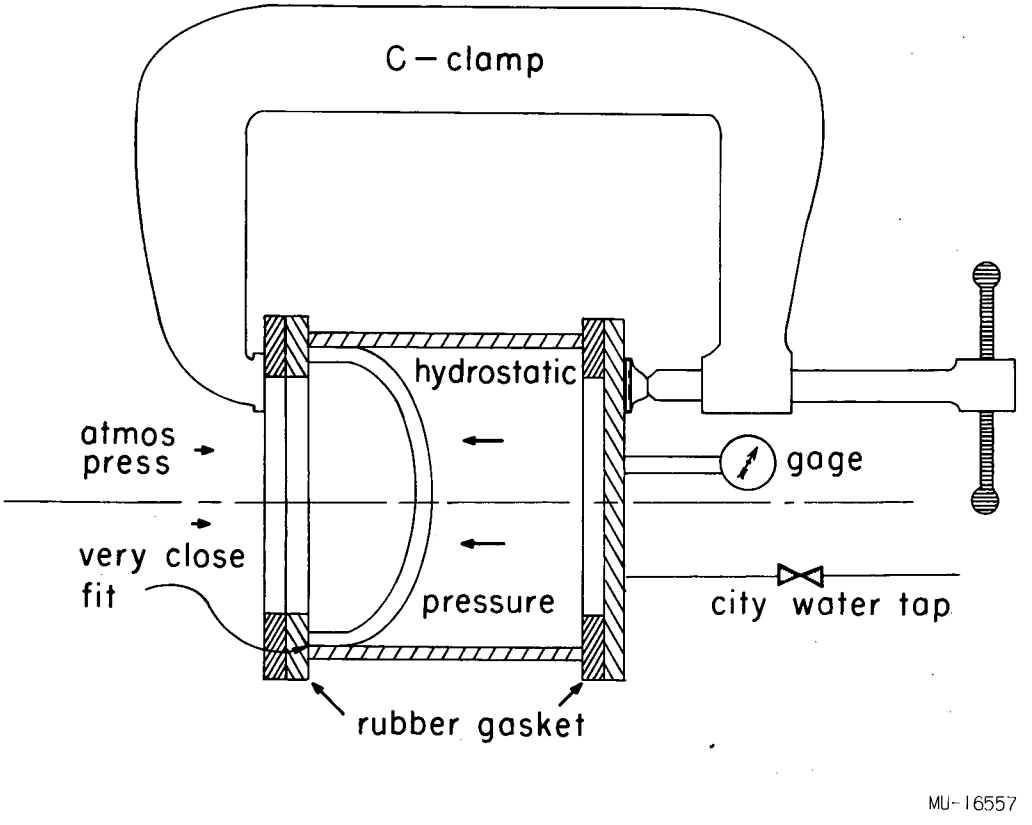

Fig. 7. Experimental arrangement for testing hydrogen-tank windows.

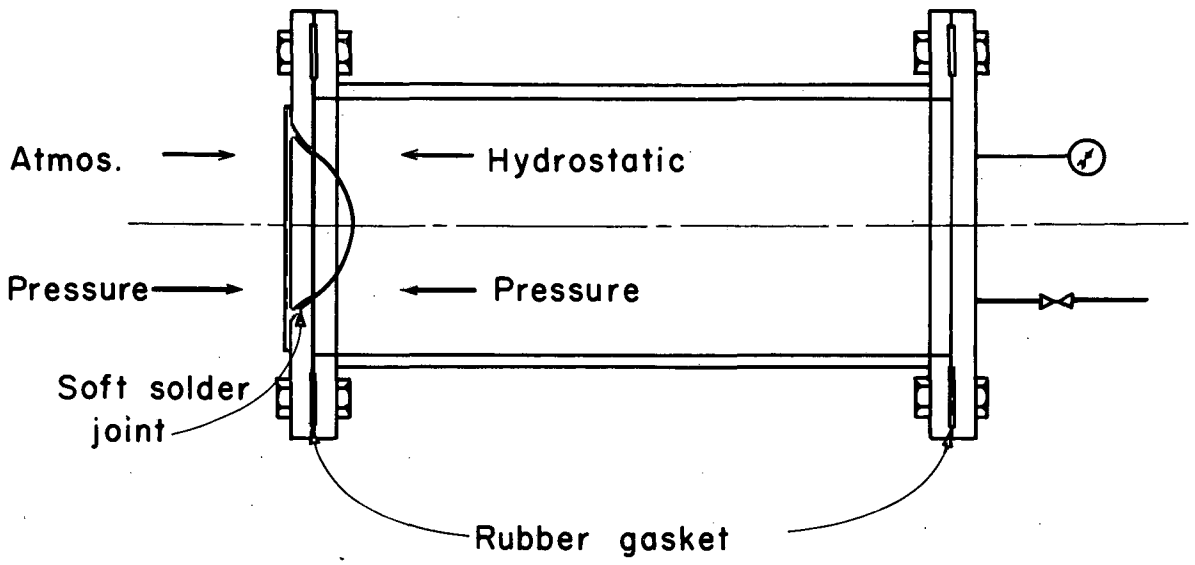

Fig. 8. Experimental arrangement for testing vacuum-jacket windows.

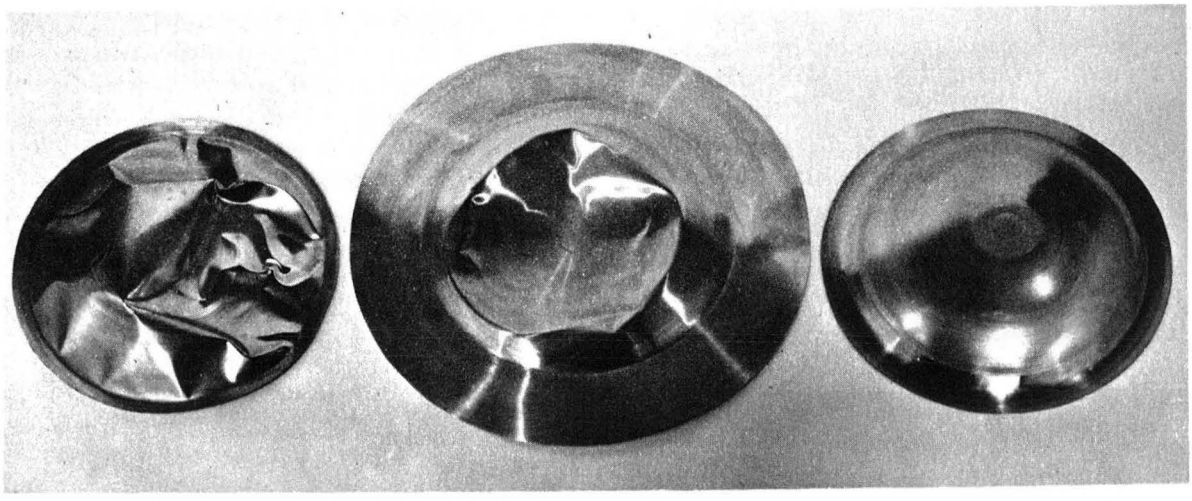

ZN-2094

Fig. 9. (right) Shell No. 6 after test.
(center) Shell No. 4 after test (flanges not trimmed).
(left) Shell No. 7 after test.

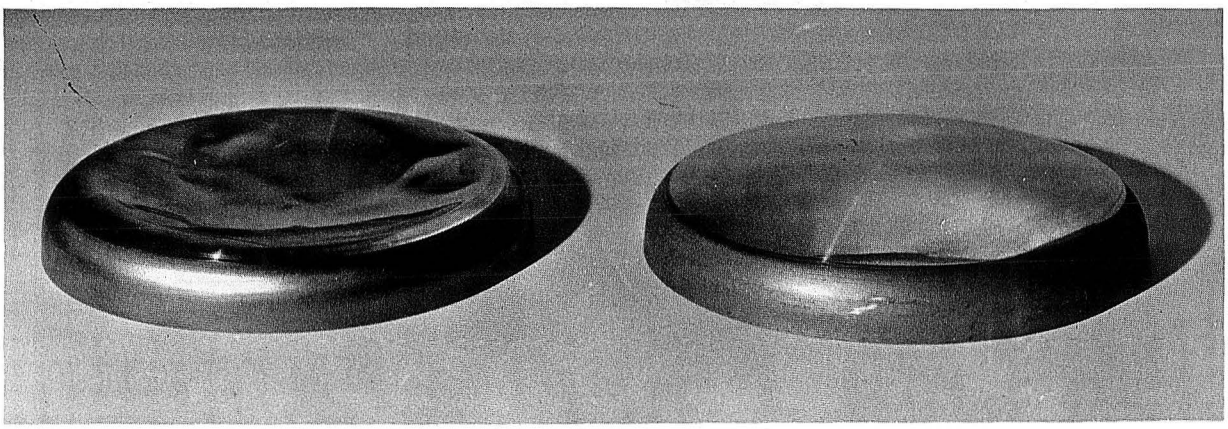

ZN-2093

Fig. 10. (right) Shell similar to No. 1. Not tested because of flaw in machining.
(left) Shell No. 2 after test.

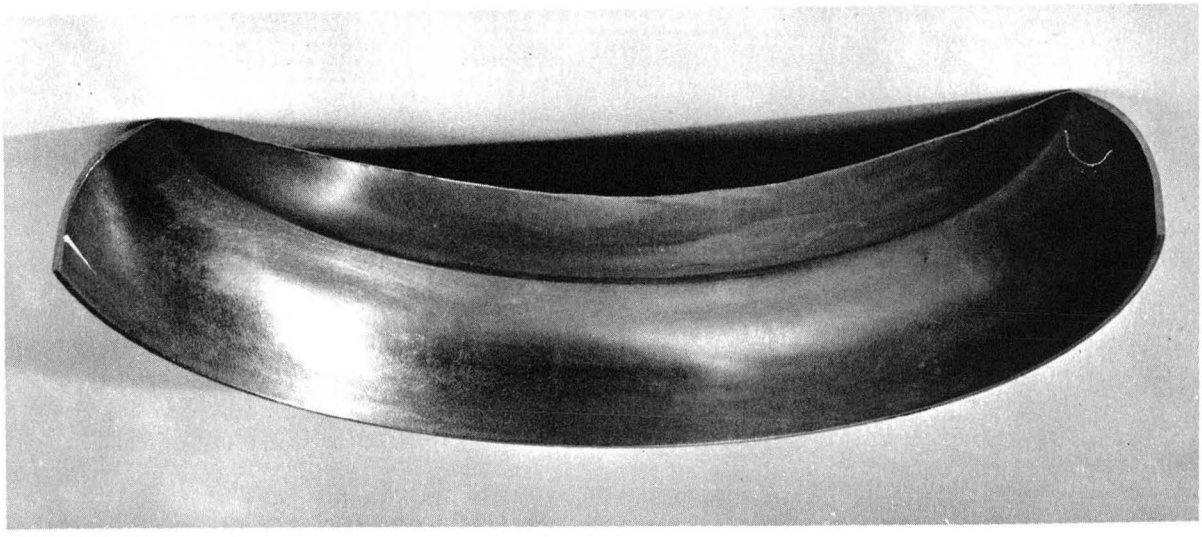

ZN-2095

Fig. 11. Cross section of shell similar to shells No. 1, 2, and 3 after test.

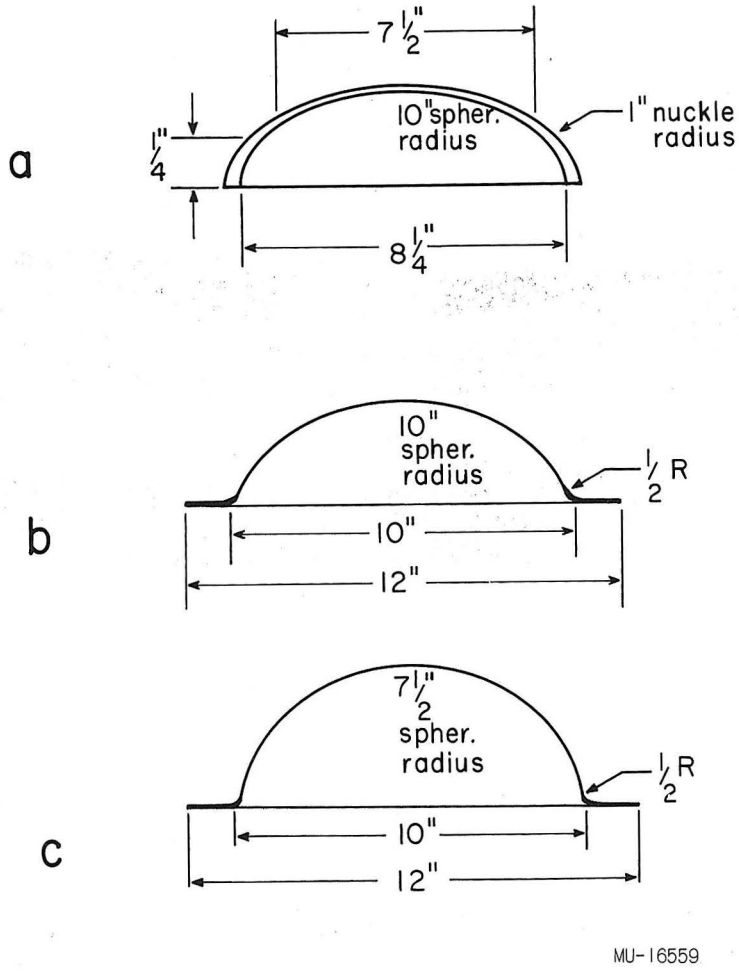

Fig 12. Dimensions of the test shells: (a) Shells No. 1, 2, and 3 were spun from 1/16-in. type-309 stainless steel, and were then machined to the required thickness; (b) Shells No. 4 and 5 were spun from type-302 stainless steel; (c) Shells No. 5 and 7 were spun from type-302 stainless steel. Shell No. 8 was spun from type-305 stainless steel.

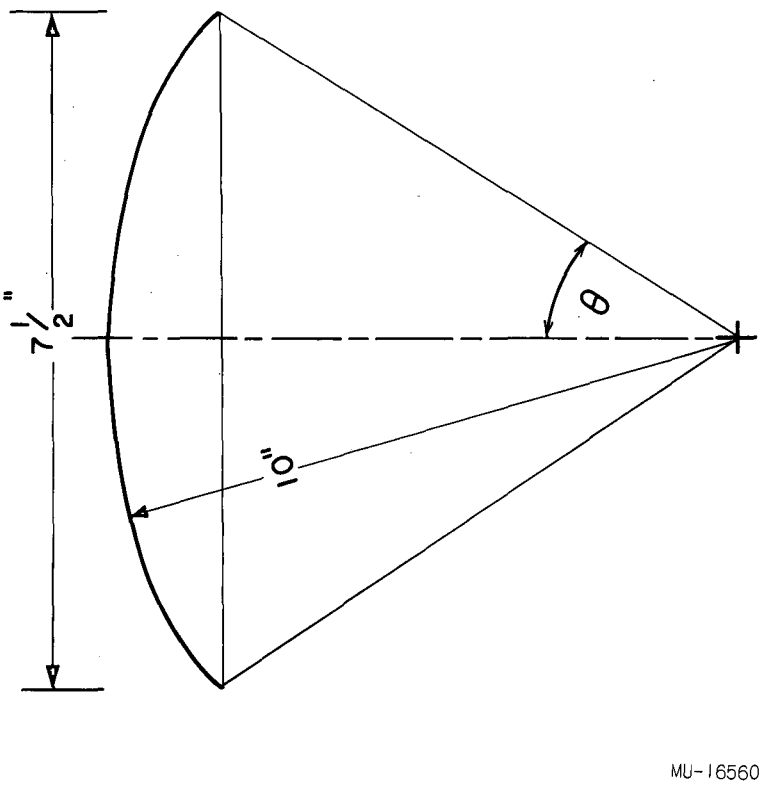

Fig. 13. Sample shell for calculations with Tsien's theory.